POLITECNICO DI TORINO
Repository ISTITUZIONALE

Single- vs. Multi-Band Optimized Power Control in C+L WDM 400G Line Systems

Original
Single- vs. Multi-Band Optimized Power Control in C+L WDM 400G Line Systems / Virgillito, E., London, E., D'Amico, A., Correia, B., Napoli, A., Curri, V.. - ELETTRONICO. - (2021), pp. 1-3. (2021 Optical Fiber Communications Conference and Exhibition, OFC 2021 San Francisco, CA, USA 6-10 June 2021).

Availability:
This version is available at: 11583/2933550 since: 2021-11-22T12:58:43Z

Publisher:
Optical Publishing Group - Institute of Electrical and Electronics Engineers Inc.

Published
DOI:

Terms of use:

This article is made available under terms and conditions as specified in the corresponding bibliographic description in the repository

Publisher copyright
Optica Publishing Group (formely OSA) postprint/Author's Accepted Manuscript

"© 2021 Optica Publishing Group. One print or electronic copy may be made for personal use only. Systematic reproduction and distribution, duplication of any material in this paper for a fee or for commercial purposes, or modifications of the content of this paper are prohibited."

(Article begins on next page)

12 November 2026

Single- vs. Multi-Band Optimized Power Control in C+L WDM 400G Line Systems

Emanuele Virgillito[(1)], **Elliot London**[(1)], **Andrea D'Amico**[(1)], **Bruno Correia**[(1)], **Antonio Napoli**[(2)], **Vittorio Curri**[(1)]

[(1)]*DET - Politecnico di Torino, Italy;* [(2)]*Infinera, Sankt-Martin-Str. 76, 81541 Munich, Germany*

emanuele.virgillito@polito.it

Abstract: We propose an optimal strategy for C+L multi-band power control assessing its performance against a single-band one. Via SSFM simulations, we demonstrate that the L-band can be optimized independently.

© 2021 The Author(s)

1. Introduction

Demand for optical network capacity and throughput will cause a geometric growth in internet traffic [1], spurred by innovations in cutting-edge end-user services such as 5G-enabled networking [2] and cloud computing solutions [3], along with traffic challenges arising from the COVID-19 era. Together with this increased capacity demand, the optical network market is moving towards the implementation of software-defined networking (SDN) and network function virtualization (NFV), allowing network orchestration and management to be automated as well as enhancing flexibility, down to the physical layer [4]. State of the art optical systems operate using wavelength-division multiplexing (WDM) within a 4.8 THz range solely in the C-band, which allows up to 64 400G-ZR+ WDM channels in the 75 GHz WDM grid. To tackle this capacity problem, multi-band systems have been proposed, extending the transmission bandwidth to the L-band and potentially towards the S-band. Multi-band transmission represents a cost-effective capacity upgrade as it utilizes already-deployed fibers with a relatively small penalty in average network traffic with respect to fiber doubling solutions [5], permitting significant capacity gains [6]. For this upgrade, the addition of transceivers and optical line amplifiers (OLAs) represents the largest CAPEX requirement. The availability of L-band amplifiers has enabled C+L systems with bandwidths up to 10 THz, at least for terrestrial long-haul segments [7]. In the C+L-band scenario stimulated Raman scattering (SRS) becomes significant due to the power transfer from higher- to lower-frequency channels (C- to L-band), along with its interaction with non-linear interference (NLI) noise generation caused by non-linear self- and cross-channel crosstalk. Consequently, in a multi-band scenario, more complex power control strategies are required to maintain the desired quality of transmission (QoT). Within this work we assume a partially disaggregated networking scenario, where reconfigurable optical add-drop multiplexer (ROADM)-to-ROADM amplified optical lines may be independent WDM optical line systems (OLSs). As in Fig.1a, from the network management perspective, a power control unit (PCU) within the OLS controller separately sets the working points for the C- and L-band OLAs. The optimum working point is determined with the aid of a QoT estimator (QoT-E). This QoT-E evaluates the generalized signal-to-noise ratio (GSNR), encompassing contributions from both the amplified spontaneous emission (ASE) noise and the NLI [4].

We focus upon the problem of power optimization when upgrading from state of the art C-band only systems to C+L, with the requirement that the previously deployed C-band remains in-service. We describe an algorithm that is used to optimize the launch power profile with respect to the QoT metric, presenting QoT estimations obtained using split-step Fourier method (SSFM) simulations to test the multi-band upgrade. We show that separately optimizing the C- and L-bands on a per-band basis enables extension to larger bands with a limited QoT penalty with respect to the optimal joint C+L multi-band power control.

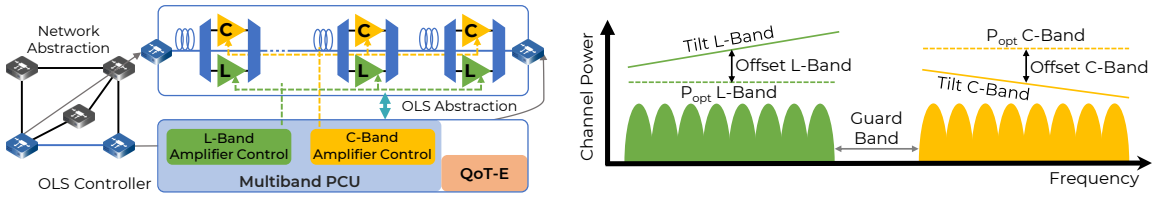

(a) (b)

Fig. 1: (a) Network and OLS representation of C+L transmission. The C- and L-bands are amplified by separate OLAs. The OLS controller implements a QoT-E module that calculates a (sub-)optimum power profile set by the PCU. (b) Representation of spectral load in C+L systems, with launch power offset and tilt used to compensate for SRS.

2. OLS Configuration and Optimization Procedure

To quantify the OLS signal quality degradation, the GSNR is commonly employed as a unique figure of merit for lightpath QoT [8], allowing contributions that arise from both linear and non-linear losses to be separately quantified. The GSNR is given by $\mathrm{GSNR}^{-1} = (\mathrm{OSNR}^{-1} + \mathrm{SNR_{NL}}^{-1})$, where the OSNR and $\mathrm{SNR_{NL}}$ are the QoT degradations due to OLAs ASE noise and NLI contributions, respectively. In order to test the C+L upgrade we have performed SSFM simulations using an internal framework [9] on an OLS consisting of 10×75 km identical spans of standard single mode fiber (SSMF), with chromatic dispersions of 16.7 ps / (nm·km) and non-linearity coefficients of $1.27\,(\mathrm{W}\cdot\mathrm{km})^{-1}$, utilizing a frequency dependent fiber loss with an average value of 0.18 dB/km. As shown in Fig.1a, the C- and L-band are amplified by EDFAs using frequency-dependent noise figures (NFs) – the NF values used within this work are obtained via device characterizations, with average values of 4.68 dB and 4.24 dB for the L- and C-bands, respectively. Each band is spectrally loaded with 64 channels, each utilizing a polarization multiplexed (PM)-16QAM transmission format and a symbol rate of $R_s = 64$ GBaud on the 75 GHz WDM grid, yielding a total of 128 channels in the C+L scenario. The C- and L-band channel combs are separated by a 500 GHz guard-band to avoid penalties due to band demultiplexing and separate amplification strategies.

To keep the impact of the SRS upon the GSNR under control, an optimization of the channel input power profile has been performed. As depicted in Fig.1b, we apply a power offset and tilt to the channel comb in each band in order to compensate for the tilt induced during propagation. These values are determined from propagation after the first fiber span, as it is assumed that the same launch power profile is recovered at each span by properly setting the EDFA gain and tilt values. The optimal power profile is found by both maximizing and flattening the GSNR of each band and is performed following a brute force approach described in [5]. The optimization procedure begins by finding the local-optimization, global-optimization (LOGO) power [11], computed separately for each spectral band; which yields $P_{opt} = -0.46$ dBm and $P_{opt} = -0.62$ dBm per channel for L- and C-bands, respectively. Next, power offset and tilt are applied for each band using the LOGO value as an initial guess; the GSNR delivered by this power configuration is evaluated by means of the generalized GN (GGN) model [10]. To find the optimal profile, all possible combinations within the problem space of all L- and C-band tilts and offsets are computed. For each configuration, the average GSNR is evaluated and all profiles within the top 1% are chosen and from these the profile with the optimal flatness value is selected. In this study, we investigated tilt values varying from -0.4 to 0.4 dB/THz with a granularity of 0.1 dB/THz. The power offset values were varied from -1.0 to 2.0 dB for the C-band and from -2.0 to 1.0 dB for the L-band, both with a granularity of 0.5 dB. The optimization algorithm has been run on four different scenarios: First, the C- and L-bands were optimized independently, i.e., considering them as a single-band system, with the former representing the typical state of an already deployed system which may be upgraded to a C+L-band scenario. We then considered C+L transmission in two cases: in the first, C- and L-bands are jointly optimized by assuming that there are no restrictions upon the tilt and offset values for either band. In the second (fourth overall) scenario, the C+L transmission is optimized with constrained tilt and offset values for the C-band, retaining the optimum single-band C-only power profile as previously set and investigating the optimum tilt and offset for L-band. This final scenario refers to a practical use case where the deployed C-band configuration must not be changed, meaning that the L-band upgrade must be performed seamlessly in order to avoid out-of-service on the deployed C-band lightpaths. The resulting optimum profiles are reported in table of Fig.2d – we note that L-band offset and tilt for both multi-band profiles are equal only incidentally, with a lower granularity in the explored parameters potentially leading to different values. The received GSNR of each obtained profile has then been estimated through SSFM simulations [9], with the results plotted in Fig.2. For each band, 7 out of 64 channels have been considered as channels under test (CUTs) and their QoT estimated. These CUTs are modulated by pseudo random binary sequence modulated channels (PRBS) to the 16^{th} degree and are received by an least mean squares (LMS)-based adaptive equalizer with 42 taps, followed by a carrier phase estimation (CPE) stage that implements a blind phase search with 16 symbols of memory.

3. Results

In Fig.2a we present the OSNR caused by the ASE noise: for all cases, its behaviour depends mostly upon the fiber loss and less upon variations within the NF. In particular, the C+L scenario with a fixed C-band optimization provides smaller OSNR due to a larger power transfer to the L-band. The NLI contribution is shown in Fig.2b: for the multi-band scenarios, the L-band performance is improved due to to negative power offset in a similar manner to how a positive offset degrades the C-band performance in the joint C+L case. The C+L, fixed C case instead shares the same profile in C-band with the single band case: the difference in the farthest channel is in fact due to the power transfer to the L-band. Considering these results from a network management perspective, we highlight some interesting considerations that arise from the final QoT metric of the GSNR, shown in Fig.2c: table of Fig.2d shows that for the system under consideration the average GSNR after 10 spans is always ≈ 20.5 dB. Furthermore, for every scenario the maximum difference with respect to the average GSNR is reported, with a

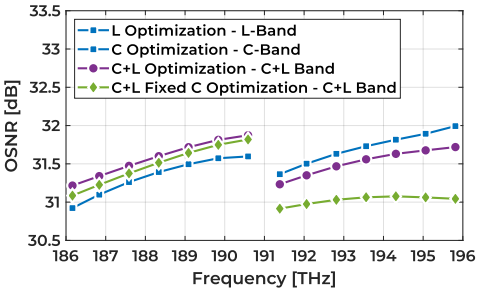

(a)

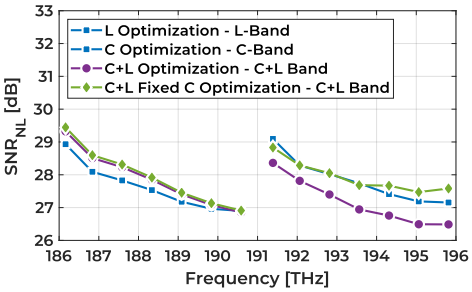

(b)

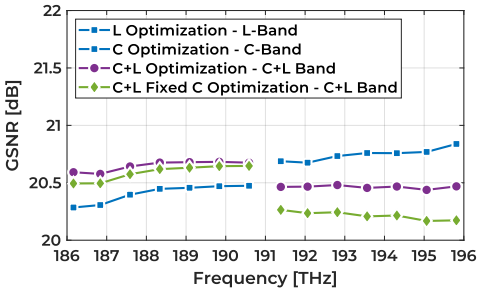

(c)

Optimization	Offset [dB]		Tilt [dB/THz]		Avg. GSNR [dB]		Max. Δ from avg GSNR [dB]	
	L	C	L	C	L	C	L	C
C-only		0.0		0.3		20.75		0.09
L-only	0.0		0.3		20.40		0.12	
Joint C+L	-0.5	0.5	0.4	0.4	20.65	20.46	0.07	0.02
C+L, Fixed C	-0.5	0.0	0.4	0.3	20.59	20.21	0.09	0.05

(d)

Fig. 2: The QoT metrics for 10×75 km spans of SSMF OLS, with 7 CUTs per band: (a) OSNR (b) SNR_{NL} (c) GSNR vs channel frequencies. In (d) we show a table reporting the offset (dB difference from the LOGO power) and tilt (dB/THz) values obtained from the input power profile optimization algorithm for single-band (C-only, L-only) and multi-band cases (Joint C+L and the C+L case where the C-band parameters are fixed). For each optimization profile the average GSNR per band and the maximum deviation from this value is reported.

value always smaller than 0.1 dB in most practical cases. For the single-band cases, the best QoT is found for the C-band, whereas the L-band benefits from C-band pumping due to SRS, causing a larger QoT in both multi-band scenarios. We remark that a joint C+L optimization enables capacity doubling at the cost of only ≈0.25 dB of penalty per 10 spans for the C-band, but requiring a change in the working points of the C-band OLAs. However, if an additional 0.25 dB of QoT penalty can be tolerated by the deployed system margins, the upgrade to C+L multiband OLS can be performed seamlessly without impairing the traffic already deployed on the C-band.

4. Conclusions

We show by SSFM simulation results that upgrading a C-band OLS consisting of 10×75 km spans of SSMF to C+L-band transmission is feasible with a minimal average GSNR penalty of only 0.25 dB in the C-band for a joint multi-band power control scenario, along with a slightly larger penalty of 0.5 dB in the case of single-band power control. We highlight that the results presented in this work hold for more general system configurations where more in-depth optimization strategies may be chosen.

Acknowledgment

This project has received funding from the European Union's Horizon 2020 research and innovation programme under the Marie Skłodowska-Curie grant agreement 814276.

References

1. Cisco Visual Networking Index: Forecast and Methodology, 2018, [Online]
2. P. Sarigiannidis, *et al*. Hybrid 5G optical-wireless SDN-based networks, challenges and open issues. *IET Networks*, 6(6), pp.141-148, 2017.
3. B. Varghese, *et al*. Next generation cloud computing: New trends and research directions. *Future Generation Computer Systems*, 79, pp.849-861, 2018
4. V. Curri. Software-defined WDM optical transport in disaggregated open optical networks. *ICTON*, pp. 1-4, 2020.
5. E. Virgillito, *et al*. Network Performance Assessment of C+L Upgrades vs. Fiber Doubling SDM Solutions. *OFC*, 2020.
6. R. Sadeghi, *et al*. Multi Bands Network Performance Assessment for Different System Upgrades. *IPC*, 2020.
7. M. Cantono *et al*. Opportunities and Challenges of C+L Transmission Systems. *JLT*, pp.1050-1060, 2019.
8. M. Filer, *et al*. Multi-vendor experimental validation of an open source QoT estimator for optical networks. *JLT*, 36(15), pp.3073-3082, 2018.
9. D. Pilori, *et al*. FFSS: The fast fiber simulator software. *ICTON*, pages 1–4. IEEE, 2017.
10. M. Cantono, *et al*. Observing the effect of polarization mode dispersion on nonlinear interference generation in wide-band optical links. *OSA Continuum*, 2(10), pp.2856-2863, 2019.
11. R. Pastorelli, *et al*. Optical control plane based on an analytical model of non-linear transmission effects in a self-optimized network. *ECOC*, pp. 1-3, 2013.